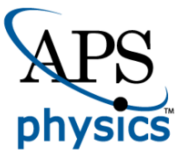

This is the accepted manuscript made available via CHORUS. The article has been published as:

Kondo Breakdown in Topological Kondo Insulators

Victor Alexandrov, Piers Coleman, and Onur Erten

Phys. Rev. Lett. **114**, 177202 — Published 28 April 2015

DOI: 10.1103/PhysRevLett.114.177202

Kondo Breakdown in Topological Kondo Insulators

Victor Alexandrov[1], Piers Coleman[1,2] and Onur Erten[1]
[1] *Center for Materials Theory, Rutgers University, Piscataway, New Jersey, 08854, USA*
[2] *Department of Physics, Royal Holloway, University of London, Egham, Surrey TW20 0EX, UK*

Motivated by the observation of light surface states in SmB_6, we examine the effects of surface Kondo breakdown in topological Kondo insulators. We present both numerical and analytic results which show that the decoupling of the localized moments at the surface disturbs the compensation between light and heavy electrons and dopes the Dirac cone. Dispersion of these uncompensated surface states are dominated by inter-site hopping, which leads to a much lighter quasiparticles. These surface states are also highly durable against the effects of surface magnetism and decreasing thickness of the sample.

Kondo insulators are a class of strongly correlated electron material in which the screening of local moments by conduction electrons gives rise to an insulating gap at low temperatures [1, 2]. The first Kondo insulator, SmB_6, discovered more than 40 years ago[3], has attracted renewed interest due to its unusual surface transport properties: while its insulating gap develops around $T_K \simeq 50$K, the resistivity saturates below a few Kelvin[4]. Although this excess conductivity was originally ascribed to mid-gap impurity states[5], renewed interest derives from the proposal that SmB_6 is a topological Kondo insulator, developing protected conducting surface states at low temperatures [6–9]. Experiments[10–13] have since confirmed that the plateau conductivity derives from surface states, and these states have been resolved by angle-resolved photoemission spectroscopy (ARPES) [14–17]. The most recent spin-ARPES experiments have also resolved the helicoidal spin polarization of the surface quasiparticles expected from topologically protected Dirac cones[18].

Yet, despite this success, certain aspects of these materials remain unexplained. A particularly notable problem, is that both quantum oscillation[19] and ARPES[13–18] studies show that the surface quasiparticles are *light*, with Fermi velocities v_s, ranging from 220meVÅ[14] to 300 meVÅ[15]; yet current theories[6–9] predict *heavy* Dirac quasiparticles with velocities $v_s \sim 30 - 50$ meVÅ, an order of magnitude slower.

Here we propose a resolution to this problem, by taking into account of the breakdown of the Kondo effect at the surface. The essence of our theory is based on the observation that the reduced co-ordination of the Sm^{3+} ions at the surface causes a marked reduction in the surface Kondo temperature $T_K^s \sim T_K/10$, so that the screening of local moments at the surface is either suppressed to much lower temperatures, or fails completely due to an intervention of surface magnetic order. "Kondo breakdown"[20–24] liberates unquenched moments at the surface, and has the effect of shifting the mixed valence of the surface Sm ions towards the higher entropy, $4f^5$ (3+) configuration of the unquenched moments, as observed in X-ray absorption spectroscopy [25]. Most importantly, Kondo breakdown will liberate a large number of carriers previously bound inside Kondo singlets at the surface (see Fig1(b) and (c)): this process localizes $4f$-holes, driving up the electron count in the surface states to form large spin-polarized Fermi surfaces determined by the Luttinger sum rule

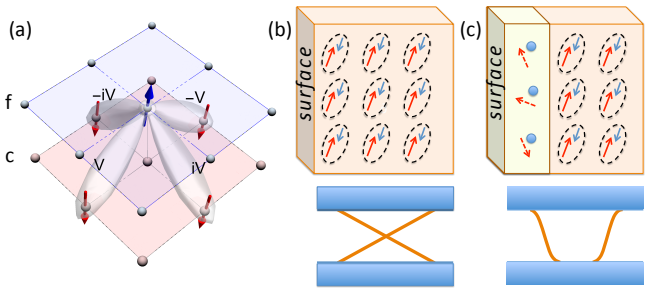

FIG. 1: (a) Schematic showing the the non-local Kondo interaction at the surface of topological Kondo insulator. The opposite parities of the f and d bands cause the hybridization to acquire a p-wave, spin-dependent form factor $\Phi(\vec{R}) \propto i\vec{R}\cdot\vec{\sigma}$ (see eq. 4), which vanishes onsite. (b) and (c) respectively contrast the surface states of a topological Kondo insulator, before and after surface Kondo breakdown, showing how the Dirac point drops into the valence band, giving rise to lighter, faster surface states.

$$\frac{\mathcal{A}_{\rm FS}}{(2\pi)^2} = \Delta n_f \qquad (1)$$

where $\mathcal{A}_{FS}$ is the total Fermi surface area of the singly-degenerate surface states, Δn_f is the change the f valence, *i.e.* for Sm $4f^{5.6+} \to 4f^{6+}$, $\Delta n_f = 0.4$, in units where the lattice constant $a = 1$. A detailed analysis presented later, shows that the dispersion of these highly doped surface states are dominated by a quadratic inter site hopping term

$$E(k_x, k_y) = E_0 + \sqrt{T_k t_f}\, r(\delta) k_\perp + t_f p(\delta) k_\perp^2, \qquad (2)$$

where t_f is the effective f hopping, while $r(\delta)$ and $p(\delta)$ are functions that depend on the surface scattering phase shift δ, as defined later. The quadratic term, absent in a conventional topological surface state, appears when the perfect compensation between heavy and light electrons

is disrupted at the surface by Kondo breakdown: this term increases the velocity of the surface states by about an order of magnitude, providing a natural explanation to the light surface states observed in experiments. Moreover, the heavy doping of the surface states shifts the Dirac point into the valence band, leading to an unusual protection of surface states against decreasing thickness and surface magnetism. We will show that the interaction of the local moments and the light surface states is described by a new kind of "chiral Kondo lattice" with the potential for a rich phase diagram of competing interacting surface states.

Model: We introduce a simplified lattice model for topological Kondo insulators, described by the periodic Anderson model:

$$H = \sum_{(i,j)\alpha,\beta} \left(d^\dagger_{i\beta}, f^\dagger_{i\beta}\right) \begin{pmatrix} -t_{ij} - \mu\delta_{ij} & \tilde{V}\Phi_{\beta\gamma}(\vec{R}_i - \vec{R}_j) \\ \tilde{V}\Phi_{\beta\gamma}(\vec{R}_i - \vec{R}_j) & \tilde{t}^f_{ij} + \tilde{\epsilon}_f\delta_{ij} \end{pmatrix} \begin{pmatrix} d_{j\gamma} \\ f_{j\gamma} \end{pmatrix} + U\sum_i n_{if\uparrow}n_{if\downarrow} \tag{3}$$

where the $d^\dagger_{j\alpha}$ and $f^\dagger_{j\alpha}$ respectively create conduction and f electrons at site j, with corresponding hopping matrix elements $-t_{ij}$ and $\tilde{t}^f_{ij}$. U is the onsite Coulomb repulsion of f-electrons. $\tilde{V}$ and $\tilde{\epsilon}_f$ are the bare hybridization and f level position. The form-factor

$$\Phi(\vec{R})_{\beta\gamma} = \begin{cases} -i\hat{R}\cdot\left(\frac{\vec{\sigma}}{2}\right)_{\beta\gamma}, & \text{n.n.} \\ 0 & \text{otherwise} \end{cases} \tag{4}$$

describes the spin-orbit coupled hybridization between neighboring f and d electrons. This simplified form factor captures the important vectorial spatial structure of hybridization between f and d states, whose orbital angular momenta differ by one unit. The hybridization is odd-parity and vanishes onsite because the heavy and light orbitals have opposite spatial parity. Fig. 1(a) shows a schematic of our model. Note that it explicitly includes an f dispersion[2], which is required for a fully gapped spectrum. Microscopically these terms are expected to result from the indirect hopping of f-electrons via the p-orbitals of the Boron ions.

To describe the large U limit we adopt a slave-boson mean-field theory and carry out a saddle point approximation in the bulk, giving rise to the mean-field Hamiltonian [26].

$$\begin{aligned} H_{MF} &= \sum_{\mathbf{k}\beta,\gamma} \left(d^\dagger_{\mathbf{k}\beta}, f^\dagger_{\mathbf{k}\beta}\right) \begin{pmatrix} \epsilon_{\mathbf{k}} - \mu & V\vec{s}_{\mathbf{k}}\cdot\vec{\sigma}_{\beta\gamma} \\ V\vec{s}_{\mathbf{k}}\cdot\vec{\sigma}_{\beta\gamma} & \epsilon_{f\mathbf{k}} + \lambda \end{pmatrix} \begin{pmatrix} d_{\mathbf{k}\gamma} \\ f_{\mathbf{k}\gamma} \end{pmatrix} \\ &+ \mathcal{N}_s(\lambda - \tilde{\epsilon}_f)\left(|b|^2 - Q\right). \end{aligned} \tag{5}$$

Here, $V = \tilde{V}b$ is the renormalized hybridization, where b is the slave boson projection amplitude. The f-hopping now becomes $t^f = b^2\tilde{t}^f$. We consider a general nearest neighbor and next nearest neighbor dispersion, $\epsilon_k = -2t\sum_i \cos k_i - 4t'\sum_{i\neq j}\cos k_i \cos k_j$ while $\epsilon_{f\mathbf{k}} = -\alpha\epsilon_k$, where, for simplicity, we have taken the ratio between the $f-$- and $d-$ electron hoppings to be a single fixed constant $\alpha = t_f/t = t'_f/t'$ for both nearest neighbor and second-neartest neighbor hoppings. The quantity λ is the constraint field that imposes the mean-field constraint $Q = n_f + b^2$, where Q is the local conserved charge associated with the slave boson treatment of the infinite U limit, here taken to be $Q = 1$; $\mathcal{N}_s$ is the total number of sites. In momentum space the form factor of the hybridization now takes the form $\Phi(\mathbf{k}) = \vec{s}_{\mathbf{k}}\cdot\vec{\sigma}$, where $\vec{s}_{\mathbf{k}} = (\sin k_x, \sin k_y, \sin k_z)$, which reduces to $\mathbf{k}\cdot\sigma$ at small k. This odd-parity hybridization is reminiscent of the gap function in topological superfluid ^{3}He-3B. This model can be regarded as an adiabatic continuation from small to large U at infinite spin-orbit coupling. Band crossing between the odd and even parity bands generates the topological band structure[27, 28] with protected surface states.

In order to obtain the surface state spectrum, we adopt Volovik's approach, mapping the reflection at the boundary onto transmission through an interface where the hybridization changes sign[29]. This method enables us to solve for the surface states using a linearized Hamiltonian. For pedagogical purposes, we take $t' = t'_f = 0$. We can treat the surface eigenstate at $k_{x,y} = 0$ as a one-dimensional problem, and since the main surface scattering effect takes place close to the Fermi surface, we can linearize the dispersion(5) normal to the surface and obtain the surface eigenstates at $k_{x,y} = 0$. The two interface eigenstates at $k_{x,y} = 0$ are given by

$$\psi_\pm \sim \begin{bmatrix} 1 \pm 1 \\ 1 \mp 1 \end{bmatrix}_\sigma \begin{bmatrix} \sqrt{\alpha} \\ \pm i \end{bmatrix}_\tau e^{-ik_z z - \kappa|z|} \tag{6}$$

where $k_z = \lambda/[t(\alpha+1)]$ and $\kappa = V/(\sqrt{\alpha}t)$. τ and σ denote the orbital and the spin component of the wave function. The corresponding energy of a state at the Dirac point is $E_0 = \lambda/(\alpha+1)$. The transverse dispersion that develops at finite $k_{x,y}$ is then treated using first order degenerate perturbation theory, projecting the full Hamiltonian H_{MF} onto the surface bound-states,

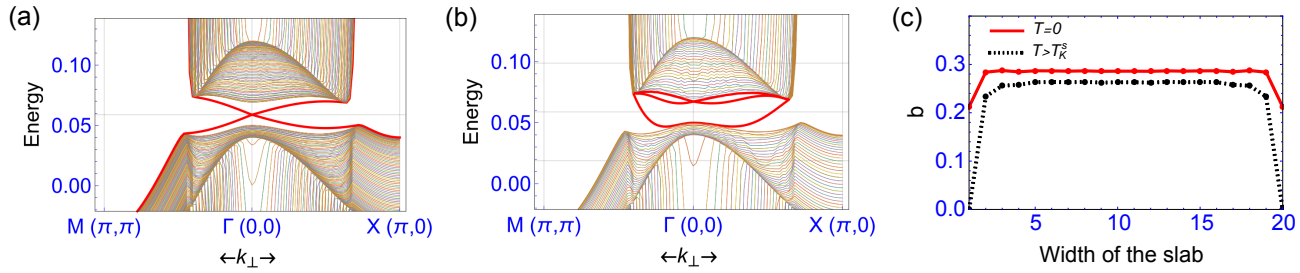

FIG. 2: Slab calculation for topological Kondo insulator: (a) for the uniform solution, (b) surface Kondo breakdown: surface local moments decouples from the rest of the system. Notice the large Fermi surface with high velocity quasiparticles in the case of the surface Kondo breakdown. (c) Inhomogeneous mean field theory calculations for the slave boson amplitude, b as a function of the thickness of the slab. b is reduced at the surface and for $T > T_K^s$, the local moments completely decouple.

$H_{eff} = \langle\psi_\pm|H_{MF}|\psi_\pm\rangle$. This leads to the dispersion

$$E(k_x, k_y) = \frac{\lambda}{\alpha+1} + 2\frac{V\sqrt{\alpha}}{\alpha+1}k_\perp + \mathcal{O}(k_\perp^3) \qquad (7)$$

where $k_\perp = \sqrt{k_x^2 + k_y^2}$. Since $\alpha \ll 1$, the surface states are composed of heavy quasiparticles. Note that at this stage, the quadratic k^2 term is absent.

Surface Kondo breakdown: The reduced co-ordination number of the f-electrons, plus the internal gapping of the bulk states lowers the effective Kondo coupling constant. If we assume crudely that the Kondo coupling constant is reduced by a factor of 5/6th, the reduced Kondo temperature is then

$$T_K = De^{-\frac{1}{J\rho}} \to T_K^s = D\exp(-\frac{6}{5J\rho}) = T_K\left(\frac{T_K}{D}\right)^{1/5} \qquad (8)$$

For example, if we take the bulk Kondo temperature $T_K \sim 50K$ with half band-width $D \sim 2eV \sim 2\times 10^4 K$, this gives a surface Kondo temperature of $T_K^s \sim 15K$. In practice, the gapping of the bulk states makes this an upper bound. This effect has been recently explored in 1D[30, 31]. However, unlike one dimension, where the spin-decoupled phase is no longer topological[30], in two and three dimensions, the topological insulator is protected by time reversal symmetry and the spin-decoupled state remains topological in the bulk. With these considerations in mind, we model the surface Kondo breakdown as the suppression of the slave boson amplitude b to zero on the surface layer of the TKI.

Surface Kondo breakdown localizes mobile f-quasiparticles at the surface, removing them from the Fermi sea. In SmB_6, this is equivalent to a shift in the effective f-valence from $4f^{5.6} \to 4f^6$ at the surface. This is a reduction in the number of f-holes, that corresponds to an increase $\Delta n_f = 0.4$ in the density of electrons on the surface. From Luttinger's sum rule (eq. 1), the area enclosed by the Fermi surface is equal to the total electron density. The Fermi surface area observed in ARPES is 0.3-0.35[13–18], in agreement with Luttinger sum rule.

Next we examine the effect of Kondo breakdown on the dispersion of the surface states. The effect of Kondo breakdown can be incorporated by introducing a scattering phase shift $\delta = k_z a$ into the f component of the surface state wave function, which ensures that surface node of the f part of the wave function is shifted one lattice unit in towards the bulk, depleting the surface of mobile f-electrons (see supplementary information for details[32]). In Volovik's approach, δ becomes a transmission phase shift. The unperturbed energy of the surface bound-state is now modified $E_0' = (\lambda + 2V\sqrt{\alpha}\sin\delta)/(1+\alpha)$ and the dispersion becomes

$$E'(k_x, k_y) = E_0' + V\sqrt{\alpha}r(\delta)k_\perp + \alpha t\frac{e^{\frac{2\kappa\delta}{k_z}} - 1}{\alpha e^{\frac{2\kappa\delta}{k_z}} + 1}k_\perp^2 \qquad (9)$$

Note the appearance of a $k_\perp^2$ term, driven by an increase the conduction electron content of the surface states. The subleading linear term is also modified, containing the renormalization $r(\delta)$ of order one: $r(\delta) = 2(\cos\delta + \frac{\kappa}{k_z}\sin\delta)/(1+\alpha\exp(\frac{2\kappa\delta}{k_z}))$. Substituting $\alpha t = t_f$ and $V \sim \sqrt{T_K t}$ in eq. 9 leads to eq. 2. This analytic result provides a natural explanation to the light quasiparticles in SmB_6. For a parameter choice of $t = 500$ meV, $t_f = 5$ meV, consistent with band structure calculations[9], and the value of $V = 100$ meV which leads to the experimentally observed gap $\Delta \simeq 20$ meV we obtain surface state velocity $v_{ss} \sim 58$ meVÅ without surface Kondo breakdown and $v_{ss} \sim 340$ meVÅ with surface Kondo breakdown in agreement with the $v_{ss} \sim 300$ meVÅ measured by ARPES experiments[15]. Here the quoted surface velocities were calculated at the mid-gap energy of the Dirac point in the absence of Kondo breakdown. We can not however, account for the much larger surface velocity $v_{ss} \sim 4000 - 7000$meVÅ reported in quantum oscillations [19].

To confirm the results of our simplified analytical calculations, we have carried out a series of slab calculations with and without Kondo breakdown. As a first check, we simulated Kondo breakdown by setting the amplitude of the surface slave boson field to zero. Without surface Kondo breakdown (Fig 2(a)), the surface states

are heavy, but as expected, when the slave boson amplitude is suppressed to zero on the surface, the topological states become much lighter as shown in Fig. 2(b). Moreover, the area of the light Fermi surface is significantly enhanced, corresponding to the extra density of carriers on the surface.

Next, to confirm that the assumption of surface Kondo breakdown we performed a fully self-consistent mean field calculation in which both $b(z)$ and $\lambda(z)$ were allowed to vary along the z direction. In this self-consistent calculation, we chose parameters where the heavy and light bands cross at the three X-points, as seen SmB_6 [14–17]; from a technical stand-point, the crossing at the three X points is required to enhance the f-character, achieving the Kondo limit $n_f \sim 1$ while still in the strong topological insulator phase. We achieve this crossing in our model by taking $t = -t'/2$, such that the heavy and light bands cross at the 3 different X points. We note that for the simpler choice $t' = 0$, bands cross at the Γ point, restricting the strong topological insulating behavior to the region to $n_f \ll 1$. Fig 2 (c) presents the results of these calculations. We find as expected, that the self-consistently determined slave boson amplitude b is depressed at the surface, corresponding to a reduction of the surface Kondo temperature. In our model calculation, for which $T_K/D \sim 0.025$ found that b^2 is depressed by $1/2$ at the surface, corresponding to $T_K^s/T_K \approx 0.5 \sim (T_K/D)^{1/5}$, a result consistent with equation (8). We also found that as the temperature is raised above the the surface Kondo temperature T_K^s, the surface b collapses to zero, even though it is still finite in the bulk. The dispersion displays a corresponding transition between heavy and light surface states as the temperature is raised through T_K^s. In practice, the possible intervention of magnetism or other instabilities may permanently prevent the low-temperature re-establishment of the Kondo effect at the surface.

Chiral Kondo lattice: The consequences of surface Kondo breakdown are rather interesting. The decoupled f-electrons now interact with the chiral surface states to form a new kind of Kondo lattice in which the conduction sea of chiral electrons is now *singly* degenerate, interacting with the local moments via a Hamiltonian

$$H_{CKL} = \sum_k \epsilon_c(k) c_k^\dagger c_k + J \sum_i \psi_i^\dagger \vec{\sigma} \psi_i \cdot \vec{S}_i + J_H \sum_{\langle ij \rangle} \vec{S}_i \cdot \vec{S}_j$$

where J is the Kondo coupling, $\vec{S}_j$ is the decoupled local moment and where $c_k^\dagger$ creates a chiral, spin polarized surface states whose dispersion $\epsilon_c(k)$ is given in eq. 9. The localized two-component electron field at site j,

$$\psi_j = \frac{1}{\sqrt{2\mathcal{N}_s}} \sum_{\mathbf{k}} \begin{pmatrix} 1 \\ \hat{k}_x + i\hat{k}_y \end{pmatrix} c_{\mathbf{k}} e^{-i\mathbf{k}\cdot\mathbf{R}_j} \qquad (10)$$

is constructed from the spin-polarized surface states by combining orbital and spin angular momentum. $J_H \sim 4t_f^2/\tilde{\epsilon}_f$ is the antiferromagnetic Heisenberg exchange between the local moments which is derived by a Schrieffer-Wolff transformation of eq. 3. The ground-state of the chiral Kondo lattice can be either magnetically ordered state or a heavy fermion liquid where the local moments are screened by chiral fermions. As in conventional heavy fermion systems, near the quantum critical point that separates these two limits, there is the possibility of strange metal behavior and superconducting ground-states. A 2D version of a similar model with 1D edge states have been explored recently[34].

Even the magnetic phase diagram of this lattice is expected to be rich. The RKKY interaction in a chiral Kondo lattice gives rise to Heisenberg, Dzyaloshniskii-Moriya and compass anisotropy terms [35] of strength J, D and A respectively. For $AJ/D^2 > 1$ the ground state is an in-plane ferromagnet whereas for $AJ/D^2 < 1$, it is a spiral of variable pitch set by D/J[36]. Such a spiral state evolves into a skyrmion crystal in applied magnetic field[37]. Experimentally, in SmB_6, indications of magnetism have been observed as hysteresis in magnetoresistance experiments[38, 39]. The absence of ordered ferromagnetic moment in XMCD experiments[25] suggests that the ground state might be a spiral with no net moment. Magnetic order breaks the time reversal symmetry and can in principle gap the surface states. We note that of the most recent single crystals show no plateau in resistivity[25] indicating that magnetism may play a crucial role in the topological behavior. Better sample quality and tuning the chiral Kondo lattice through a quantum critical point opens up the possibility of exotic superconductivity on the surface of topological Kondo insulators.

Thickness dependence of surface states: Perfect topological protection of the surface states requires an infinite bulk. When the thickness of the system is comparable to the decay length, $\xi = \kappa^{-1}$ of the surface states, the two surface states on each surface mix, giving rise to a gap in the spectrum. Since the mixing is a zero-momentum transfer process, the gap opens at the doubly degenerate Dirac point as shown in Fig. 3(a). This effect has been observed in conventional topological insulators like Bi_2Se_3 where the surface states get gapped for thickness 3-5 quintuple layers[40]. However with surface Kondo breakdown, the Dirac point shifts in the valence band, giving rise to a unique protection against decreasing thickness of the sample (Fig. 3(b)). Recent transport experiments on films about L=100-200nm thicknesses observe topological surface states [41]. We predict that the topological states will persist even in ultra-thin samples, $L \sim \xi \sim 10nm$, making SmB_6 a perfect candidate for thin film applications. This mechanism also gives rises to protection against small time reversal symmetry breaking effects such as weak magnetism at the surface.

Conclusion: To conclude, we have addressed the origin of the light surface states of topological Kondo insulators as

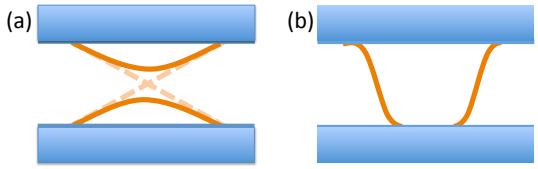

FIG. 3: (a) Without the surface Kondo breakdown, the surface states are susceptible to reducing thickness and and effects of magnetism where an insulating gap starts developing around the Dirac point. (b) In the case of surface Kondo breakdown, the Dirac point sinks in the valence band, providing an unusual protection to the surface states. The spectrum stays metallic and qualitatively unchanged for moderate values of perturbation.

a simple consequence of surface Kondo breakdown. Our results appear to reconcile the observation of light surface states and the peculiar shift of valence in Sm observed in X-ray measurements. This theory also predicts an increased stability of the the surface states against finite thickness and magnetism may be important in thin film device fabrication. We have also argued that the interaction of the surface spins with spin-polarized light surface states is described by a chiral Kondo lattice: a two dimensional Kondo lattice with strong parity violation, with the potential for a rich phase diagram in the vicinity of its magnetic quantum critical point. The detailed character of the surface states at low temperatures, with the possibility of a wide variety of magnetic or other orderings [42, 43] remains a fascinating topic for future research.

Acknowledgments: We gratefully acknowledge stimulating conversations with Jim Allen, Tzen Ong, Kai Sun, George Sawatzky and David Vanderbilt. This work is supported by Department of Energy grant DE-FG02-99ER45790.

[1] Z. Fisk *et al.*, Physica B **206 & 207**, 798 (1995).
[2] P. Coleman, *Handbook of Magnetism and Advanced Magnetic Materials* (John Wiley and Sons, Ltd., 2007).
[3] A. Menth, E. Buehler, and T. H. Geballe, Phys. Rev. Lett. **22**, 295 (1969).
[4] J. W. Allen, B. Batlogg, and P. Wachter, Phys. Rev. B **20**, 4807 (1979).
[5] J. C. Nickerson *et al.*, Phys. Rev. B **3** (1971).
[6] M. Dzero, K. Sun, V. Galitski, and P. Coleman, Phys. Rev. Lett. **104**, 106408 (2010).
[7] M. Dzero, K. Sun, P. Coleman, and V. Galitski, Phys. Rev. B **85**, 045130 (2012).
[8] V. Alexandrov, M. Dzero, and P. Coleman, Phys. Rev. Lett. **111**, 226403 (2013).
[9] F. Lu *et al.*, Phys. Rev. Lett. **110**, 096401 (2013).
[10] S. Wolgast *et al.*, Phys. Rev. B **88**, 180405 (2013).
[11] X. Zhang *et al.*, Phys. Rev. X **3**, 011011 (2013).
[12] D. J. Kim *et al.*, Scientific Reports **3**, 3150 (2013).
[13] D. J. Kim, J. Xia, and Z. Fisk, Nature Materials **13**, 466 (2014).
[14] J. Jiang *et al.*, Nat. Comm. **4**, 3010 (2013).
[15] M. Neupane *et al.*, et al., Nat. Comm. **4**, 2991 (2013).
[16] N. Xu *et al.*, Phys. Rev. B **88**, 121102 (2013).
[17] E. Frantzeskakis, N. de Jong, B. Zwartsenberg, Y. K. Huang, Y. Pan, X. Zhang, J. X. Zhang, F. X. Zhang, L. H. Bao, O. Tegus, et al., Phys. Rev. X **3**, 041024 (2013).
[18] N. Xu, P. K. Biswas, J. H. Dil, G. Landolt, S. Muff, C. E. Matt, X. Shi, N. C. Plumb, M. Radavic, E. Pomjakushina, et al., Nature Comm. **5**, 4566 (2014).
[19] G. Li *et al.*, arXiv p. 1306.5221 (2013).
[20] Q. Si, S. Rabello, K. Ingersent, and J. L. Smith, Nature **413**, 804 (2001).
[21] P. Coleman, C. Pépin, Q. Si, and R. Ramazashvili, J. Phys.: Condens. Matter **13**, 723 (2001).
[22] T. Senthil, S. Sachdev, and M. Vojta, Phys. Rev. Lett. **90**, 216403 (2003).
[23] C. Pépin, Phys. Rev. Lett. **98**, 206401 (2007).
[24] I. Paul, C. Pépin, and M. Norman, Phys. Rev. Lett. **98**, 026402 (2007).
[25] W. A. Phelan *et al.*, Phys. Rev. X **4**, 031012 (2014).
[26] P. Coleman, Phys. Rev. B **35**, 5072 (1987).
[27] M. Z. Hasan and C. L. Kane, Rev. Mod. Phys. **82**, 3045 (2010).
[28] X.-L. Qi and S.-C. Zhang, Rev. Mod. Phys. **83**, 1057 (2011).
[29] G. E. Volovik, JETP Letters **90**, 398 (2009).
[30] V. Alexandrov and P. Coleman, Phys. Rev. B **90**, 115147 (2014).
[31] A. M. Lobos, A. O. Dobry, and V. Galitski, arXiv p. 14115357 (2014).
[32] See Supplemental Material [url], which includes Ref. [33].
[33] N. Andrei, K. Furuya, and J. Lowenstein, Rev. Mod. Phys **55**, 331 (1983).
[34] B. L. Altshuler, I. L. Aleiner, and V. I. Yudson, Phys. Rev. Lett. **111**, 086401 (2013).
[35] J.-J. Zhu, D.-X. Yao, S.-C. Zhang, and K. Chang, Phys. Rev. Lett. **106**, 097201 (2011).
[36] S. Banerjee, O. Erten, and M. Randeria, Nat. Phys **9**, 626 (2013).
[37] S. Banerjee, J. Rowland, O. Erten, and M. Randeria, Phys. Rev. X **4**, 031045 (2014).
[38] Y. Nakajima *et al.*, arXiv p. 1312.6132 (2013).
[39] Y.-S. Eo *et al.*, arXiv p. 14107430 (2014).
[40] Y. Zhang *et al.*, Nat. Phys. **6**, 584 (2010).
[41] J. Yong *et al.*, arXiv p. 1408.5413 (2014).
[42] D. K. Efimkin and V. Galitski, Phys. Rev. B **90**, 081113 (2014).
[43] B. Roy *et al.*, arXiv p. 14101868 (2014).